



Cortical and subcortical grey matter atrophy in Amyotrophic Lateral Sclerosis correlates with measures of disease accumulation independent of disease aggressiveness

Nora Dieckmann^a, Annekathrin Roediger^a, Tino Prell^b, Simon Schuster^c, Meret Herdick^c, Thomas E. Mayer^d, Otto W. Witte^a, Robert Steinbach^{a,*},^{1,2}, Julian Grosskreutz^{c,1}

^a Department of Neurology, University Hospital Jena, Jena, Germany

^b Department of Geriatrics, University Hospital Halle, Halle, Germany

^c Precision Neurology, University of Lübeck, Luebeck, Germany

^d Department of Neuroradiology, University Hospital Jena, Jena, Germany

ARTICLE INFO

Keywords:

Amyotrophic Lateral Sclerosis
MRI
Biomarkers
Cortical Thickness
D50-model
CAT12

ABSTRACT

There is a growing demand for reliable biomarkers to monitor disease progression in Amyotrophic Lateral Sclerosis (ALS) that also take the heterogeneity of ALS into account.

In this study, we explored the association between Magnetic Resonance Imaging (MRI)-derived measures of cortical thickness (CT) and subcortical grey matter (GM) volume with D50 model parameters.

T1-weighted MRI images of 72 Healthy Controls (HC) and 100 patients with ALS were analyzed using Surface-based Morphometry for cortical structures and Voxel-based Morphometry for subcortical Region-Of-Interest analyses using the Computational Anatomy Toolbox (CAT12). In Inter-group contrasts, these parameters were compared between patients and HC. Further, the D50 model was used to conduct subgroup-analyses, dividing patients by a) Phase of disease covered at the time of MRI-scan and b) individual overall disease aggressiveness. Finally, correlations between GM and D50 model-derived parameters were examined.

Inter-group analyses revealed ALS-related cortical thinning compared to HC located mainly in frontotemporal regions and a decrease in GM volume in the left hippocampus and amygdala. A comparison of patients in different phases showed further cortical and subcortical GM atrophy along with disease progression. Correspondingly, regression analyses identified negative correlations between cortical thickness and individual disease covered. However, there were no differences in CT and subcortical GM between patients with low and high disease aggressiveness.

By application of the D50 model, we identified correlations between cortical and subcortical GM atrophy and ALS-related functional disability, but not with disease aggressiveness. This qualifies CT and subcortical GM volume as biomarkers representing individual disease covered to monitor therapeutic interventions in ALS.

1. Introduction

Amyotrophic Lateral Sclerosis (ALS) is a progressive neurodegenerative disease and survival rates are short with patients succumbing three

years after the onset of symptoms on average (Kiernan et al., 2011; Longinetti and Fang, 2019; van Es et al., 2017). There is marked heterogeneity in terms of different disease onsets, patterns of clinical spread of symptoms, and most of all vastly differing disease progression-speed

Abbreviations: ALS, Amyotrophic Lateral Sclerosis; ALSFRS-R, ALS Functional Rating Scale (Revised); CAT12, Computational Anatomy Toolbox; cFL, Calculated Functional Loss-rate; cFS, Calculated Functional State; CT, Cortical Thickness; D50, disease aggressiveness; GM, Grey Matter; HC, Healthy Controls; MRI, Magnetic Resonance Imaging; rD50, relative D50 (individual disease covered); PrCG, Precentral Gyrus; ROI, Region-Of-Interest; SBM, Surface-based Morphometry; SPM, Statistical Parametric Mapping; TIV, Total Intracranial Volume; VBM, Voxel-Based Morphometry; WM, White Matter.

* Corresponding author at: Hans Berger Department of Neurology, University Hospital Jena, Am Klinikum 1, 07747 Jena, Germany.

E-mail address: Robert.Steinbach@med.uni-jena.de (R. Steinbach).

¹ These authors contributed equally.

² ORCID-Id: 0000-0003-3936-6010.

<https://doi.org/10.1016/j.nicl.2022.103162>

Received 30 January 2022; Received in revised form 11 July 2022; Accepted 18 August 2022

Available online 22 August 2022

2213-1582/© 2022 The Authors. Published by Elsevier Inc. This is an open access article under the CC BY-NC-ND license (<http://creativecommons.org/licenses/by-nc-nd/4.0/>).

(Westeneng et al., 2018). This impairs the comparability of ALS cohorts and challenges monitoring disease progression in clinical trials (Kiernan et al., 2021). Therefore, reliable biomarkers are needed that allow continuous and objective assessment of ALS pathology and progression.

The opportunity of neuroimaging to support diagnostics, staging, and therapeutic monitoring in ALS, led to international joint efforts, notably the Neuroimaging Society in Amyotrophic Lateral Sclerosis (NiSALS) (Turner et al., 2011). Nevertheless, discrepancies remain between the measurements derived from Magnetic Resonance Imaging (MRI) and the individual ALS disease course (Steinbach et al., 2018; Verstraete et al., 2015). Many of these studies used the ALS Functional Rating Scale Revised (ALSFRS-R) or the disease duration as singularly assessed indicators of clinical disease burden. However, some could not reveal any correlation between these markers of disability and MRI-derived measures of Cortical Thickness (CT) analyses (de Albuquerque et al., 2017; Schuster et al., 2014), whilst others described correlations occurring in single cortical areas (d'Ambrosio et al., 2014; Kwan et al., 2012; Spinelli et al., 2020). Reasons for these inconsistencies could be attributed to 1) the heterogeneous biological basis of ALS, 2) the differences and limitations of the used imaging techniques and analyzes, and 3) the inaccuracies of clinical measures.

For the latter, the D50 disease progression model was developed to overcome such limitations of traditional clinical metrics and has already proven to facilitate robust correlations with values originating from structural MRI analyses as well as other biomarkers (Dreger et al., 2021; Magen et al., 2021; Steinbach et al., 2021a). Briefly, the D50 model describes overall disease aggressiveness as the time taken to reach halved functionality (D50) and further enables the calculation of individual disease covered (e.g., in distinct phases) and of acute descriptors of local disease activity. A strength of the D50 model in comparison to traditional disease metrics, e.g., the linearly approximated disease progression-rate, is that it takes into account the individual clinical course as a whole and reflects its typically curvilinear decline of disability more appropriately (Gordon et al., 2010; Thakore et al., 2018). It describes the accumulating loss of motoric functions over time as a sigmoidal curve from full health to functional loss.

Applying this model, we demonstrated that grey matter (GM) alterations, as assessed via Voxel-Based Morphometry (VBM) (Ashburner and Friston, 2000), are sequentially worsening and spreading into several brain regions with increasing disease covered in ALS (Steinbach et al., 2020; Steinbach et al., 2021b). In contrast, GM structures did not correlate with disease aggressiveness, as quantified by the D50-value. In principle, this qualifies assessments of GM structural integrity to serve as a marker of disease accumulation in ALS, independent of disease aggressiveness. However, on a continuous level, correlations between disease accumulation and VBM measures of GM structures were lacking, as suggested in other studies before (Agosta et al., 2007; Menke et al., 2014).

This might be partly explained by the limitations of the VBM method. It is susceptible to segmentation failures, thus resulting in less accurate classifications as compared to CT-based methods (Jiao et al., 2010; Pereira et al., 2012). Surface-based Morphometry (SBM) has the advantage to decompose cortical volume into thickness, gyrification, and surface area and is, therefore, more reliable for cortical topology (Turner et al., 2012). Several studies using SBM were able to reveal patterns of cortical atrophy in ALS (Schuster et al., 2013; Verstraete et al., 2010; Verstraete et al., 2012) and CT seemed to be more sensitive to upper motoneuron involvement and disease-related changes in ALS than VBM (Turner et al., 2012; Turner and Verstraete, 2015). Of note, GM changes in ALS disease are not limited to cortical or motoric structures (Bede et al., 2013; Westeneng et al., 2015).

In this study, we aimed to determine if and how the integrity of cortical and subcortical GM can be used as a neuroimaging biomarker in ALS. We hypothesized that decreasing CT and/or subcortical volume are a continuous, one-directional process during the course of the disease. The D50 disease progression model was applied here to probe such

direct correlations of accumulated disease/disease covered with SBM metrics of GM integrity for the first time. We further postulated that these GM measures are independent of disease aggressiveness, thus exclusively reflecting the ongoing accumulation of ALS pathology. Having a suitable biomarker fulfilling these criteria of being specific for the amount of disease covered, whilst being independent of disease aggressiveness would be an essential step towards using MRI to monitor effectiveness of therapeutic interventions.

2. Methods

2.1. Subject identification

All patients were recruited from the center for neuromuscular and motoneuron diseases at Jena University Hospital (Jena, Germany). All participants signed written informed consent prior to the commencement of the study. All experiments were approved by the local Ethics Committee of the Friedrich Schiller University in Jena (3633–11/12) and conducted in accordance with the Declaration of Helsinki and its later amendments.

In first instance, 162 patients were identified from a prospectively recruited cohort study. All patients received MRI via the same harmonized protocol, acquired in a scanner used for clinical routine diagnostics. They all fulfilled the revised El Escorial criteria for definite, probable, or probable laboratory-supported ALS (Brooks et al., 2000). All patients were examined and diagnosed by a neurodegenerative specialist before the commencement of the study and in follow-up visits. Patients fulfilling the following criteria were excluded from this cohort of ALS patients: 1) juvenile ALS, 2) primary lateral sclerosis, 3) manifest dementia, or 4) other comorbidities that could affect motor performances. In a next step, we also excluded patients with cognitive deficits or unavailable/incomplete cognitive testing according to neuropsychological screening assessments. For patients enrolled before 2015, these were Mini-Mental State Examination <26 points (Creavin et al., 2016) and/or frontal assessment battery <13.5 points (Appollonio et al., 2005; Dubois et al., 2000). For patients enrolled after 2015 the Edinburgh Cognitive and Behavioral Amyotrophic Lateral Sclerosis Screen (ECAS) was used with German education and age-adjusted cutoffs (Abrahams et al., 2014; Lule et al., 2015).

Consequently, 110 patients with ALS could be identified for this study (for a CONSORT diagram please refer to [Supplementary Fig. S1](#)).

Healthy Controls (HC) were recruited from whole population and did not suffer from any morbidities affecting either cognitive or motoric functions.

2.2. Clinical characterization of patients

The D50 disease progression model was developed to provide a quantifiable characterization of the individual ALS disease course and thereby overcome disadvantages of traditional disease metrics such as noise or rater-variability (Bakker et al., 2020; Gordon et al., 2010). It describes the disease state transition as a sigmoidal curve and is calculated by iterative fitting of regularly gathered ALSFRS-R scores for each patient. Interested readers may also refer to Dreger et al. (2021) or Steinbach et al. (2021a). The D50-value itself is defined as the estimated time taken in months after onset of symptoms until a patient loses half of his motoric functions. Thus, D50 is a descriptor of the individual overall disease aggressiveness. A lower D50 value reflects a more aggressive form of the disease, meaning that it takes less time until halved functionality. For subgroup comparison of patients with different forms of disease, they were subdivided into having an overall low aggressive (D50 > 30 months) or high aggressive (D50 ≤ 30 months) ALS.

Normalizing the D50-value onto 0.5 yields the relative D50 (rD50) which allows comparability of differing disease courses of patients. rD50 measures individual disease covered, independent of disease aggressiveness, where 0 represents the symptom onset and 0.5 equals the time

point of halved functionality. Based on rD50, the disease course can be divided into distinct phases: a) the early semi-stable Phase I ($rD50 < 0.25$), b) the early progressive Phase II ($0.25 \leq rD50 < 0.50$), and c) the late progressive/stable Phases III/IV ($rD50 \geq 0.50$). In this study patients were subdivided according to their individual rD50 at the time of MRI, as either being in Phase I ($rD50 < 0.25$) or in higher phases ($0.25 \leq rD50$).

Besides, descriptors of local disease activity can be calculated for any given time point, namely the calculated Functional State (cFS) and the calculated Functional Loss-rate (cFL). The cFS uses the same scale as the ALSFRS-R score, the cFL measures the acute decay rate of points lost per month for any given point in time, e.g., at MRI. Thus, the model provides information about disease accumulation (rD50 and cFS) and the acute disease activity (cFL) at time points where no original ALSFRS-R was acquired which was particularly useful for patients in our cohort who were not scored with the ALSFRS-R close to MRI-scanning.

2.3. MRI processing

2.3.1. MRI acquisition and preprocessing

MRI-scans were performed with a 1.5 Tesla Siemens Sonata Scanner at Jena University Hospital with a FLASH 3D sequence acquiring 192 sagittal slices (repetition time = 15 ms, echo time = 5 ms, Flip Angle = 30° , FOV 240 mm * 256 mm, slice thickness 1 mm, pixel size 1 mm * 1 mm) using a standard 4-channel head coil. The original T1-weighted DICOM images were then converted into Nifti format using Dcm2Nii (MRICroN).

All T1-weighted and FLAIR raw images (acquired in the same scanning session) underwent visual inspection for artifacts (done by RS). Preprocessing and analysis of images was conducted with the CAT12-Toolbox (version 12.7; <https://dbm.neuro.uni-jena.de/cat/>) as implemented in SPM12 (version v7771 for MRI/VBM data on Windows; Wellcome Trust Centre for Neuroimaging; <https://fil.ion.ucl.ac.uk/spm/software/spm12/>) on Matlab2020a Surface. The steps of preprocessing followed the CAT12 standard pipeline using default settings unless indicated otherwise.

The images were segmented into white matter (WM), grey matter (GM) and Cerebrospinal Fluid. Following, a second quality assurance was conducted using the “Check homogeneity function” in CAT12 and potential outliers were again visually inspected (done by ND and RS). Ten patients were excluded due to segmentation failure or insufficient image quality and finally the images of 100 patients with ALS could be used for further analyzes. The images of all 72 HC fulfilled the quality criteria for this study.

2.3.2. Cortical thickness

Surface parameters were extracted using the SBM functions in CAT12 (“Surface Tools > Extract Surface Parameters”) which calculates quantitative measures of cortical GM such as Cortical Thickness (Frangou et al., 2022). An advantage of SBM is that accuracy of brain registration has proven to be higher than in VBM methods (Anticevic et al., 2008) and by inflation and spherical mapping blurred sulci can be brought to the surface (Dahnke et al., 2013). CT was estimated in one step using a project-based distance measure (Dahnke et al., 2013). Measures were resampled and smoothed with a 15 mm full-width at half maximum Gaussian Kernel as described before (Spalthoff et al., 2018). No absolute masking threshold was applied, as recommended in the CAT12 manual.

2.3.3. Regions-Of-Interest

Besides whole-brain vertex-wise analyses of surface parameters, Region-Of-Interest (ROI) analyses of subcortical GM structures were performed. To correct for different brain sizes, we estimated the Total Intracranial Volume (TIV) (“CAT12 > Statistical Analysis > Estimate TIV”), which was applied in all ROI-analyses as a nuisance covariate. The segmented GM images were smoothed with an 8 mm full-width at half maximum kernel (with SPM12 module “Smooth”). The 22 ROIs per

hemisphere were defined based on the CoBra-Atlas (Entis et al., 2012; Park et al., 2014; Tullo et al., 2018; Winterburn et al., 2013). These consisted of bilateral thalamus, amygdala, hippocampus (with subfields CA1, CA2/3, CA4/dentate gyrus, stratum radiatum/ stratum lacunosum/stratum moleculare, and subiculum) globus pallidus, striatum, and the cerebellum (divided into 13 subregions per hemisphere).

2.3.4. Statistical analysis

The specification of 2nd-level models and further check for homogeneity and design orthogonality was done using full-factorial model designs for cross-sectional data (“Basic Module” function in CAT12). By checking design orthogonality, we assured that there were no considerable correlations between the different parameters of interest and calculated parameters TIV and CT in our analyses.

First, we tested for inter-group differences between patients and HC, using age and gender as nuisance covariates. Within the group of patients with ALS, subgroup contrasts were calculated for a) Phase I (early stable Phase: $rD50 < 0.25$) versus higher phases ($0.25 \leq rD50$), and b) low disease aggressiveness ($D50 \geq 30$ months) versus high disease aggressiveness ($D50 < 30$ months). Further, regression analyses were performed with the modeled parameters rD50, D50, cFL, and cFS. In analyses between subgroups of patients and regression contrasts, we applied disease onset (bulbar/spinal) and the congruent parameter to our parameter of interest as nuisance covariates. For example, for the comparison of rD50-derived phases, type of onset and D50 were considered covariates; or for the regression with cFL, onset-type and cFS were included in the design. TIV was additionally included as nuisance covariate in all ROI-analyses. For CT-analyses the significance level was set at $p < 0.001$ and a cluster extent threshold at the number of expected vertices per cluster was applied (Woo et al., 2014). Analyzing subcortical ROI volumes, the significance level was set at $p < 0.05$ Holm-Bonferroni corrected.

Statistical analyses of demographic and clinical data were performed using the SPSS® software program (IBM®, v27.0.0.0). Non-normal distribution of all demographic and clinical variables was confirmed using the Shapiro Wilks test. Metric variables are expressed as mean with standard deviation, skewed variables as median with interquartile-range and categorical variables as absolute numbers. Comparison of groupwise means was appropriately conducted either with a two-sample *t*-test, a Mann-Whitney-*U* test, or chi-square-test.

3. Results

3.1. Study cohort

Detailed clinical and demographic data for patients with ALS are given in Table 1. There were no significant differences in distribution of gender (ALS: 45 female; HC: 38 female; $p = 0.314$) or handedness (ALS: 93 right-handed; HC: 64 right-handed; $p = 0.803$) between patients and HC. Patients were significantly older than HC (ALS: 64.17 ± 16.77 ; HC: 53.87 ± 14.28 ; $p < 0.001$). Patients in higher rD50-derived phases were older than those in Phase I (Phase I: 61.46 ± 15.96 ; higher phases: 66.37 ± 12.45 ; $p = 0.01$; for further information see Supplementary Table S1). There was no significant difference in age between patients with different levels of disease aggressiveness (for further information see Supplementary Table S2).

3.2. Comparison between ALS patients and HC

SBM revealed 15 clusters with significant cortical thinning in ALS as compared to HC. These clusters were located in multiple areas of the brain, predominantly in frontotemporal regions: bilateral superior frontal gyri, superior and medial temporal gyrus, left medial frontal gyrus, left temporal pole, and left precentral sulcus ($p < 0.001$; Fig. 1A). There were no clusters with increased CT in ALS in comparison to HC.

The subcortical ROI-analyses also revealed ALS-related significant

Table 1
Demographic and clinical data for patients with ALS.

Characteristics	ALS, n = 100
<i>Demographic</i>	
Age at MRI [years] #	64.17 ± 16.77 (32.75–81.41)
Gender [male/female] ⊕	55/45
Handedness [left/right/unknown] ⊕	93/6/1
<i>Neurocognitive Screening</i>	
ECAS	for n = 68
- ECAS total score [points] ⊠	152.76 ± 21.39 (100–192)
- ALS-specific subscore ⊠	74.22 ± 10.91 (46 – 96)
- ALS Non-specific subscore ⊠	78.54 ± 10.63 (54 – 96)
FAB	for n = 33
- FAB Total score [points] ⊠	17.48 ± 0.87 (15–18)
MMSE	for n = 35
- MMSE Total score [points] ⊠	29.29 ± 1.02 (26–30)
<i>Disease Metrics</i>	
Symptom Duration [months] #	13 ± 12 (4–59)
onset [bulbar/spinal] ⊕	33/67
D50 [months] #	30.04 ± 19.78 (6.04–96.20)
Low Aggressiveness (D50 ≥ 30) ⊕	51
High Aggressiveness (D50 < 30) ⊕	49
relative D50 (rD50) ⊠	0.26 ± 0.12 (0.05–0.52)
Phase I at MRI (rD50 < 0.25) ⊕	48
higher phases at MRI (0.25 ≤ rD50) ⊕	52
- Phase II (0.25 ≤ rD50 ≤ 0.50)	49
- Phases III/IV (0.50 ≤ rD50)	3
cFS [points] ⊠	38.80 ± 6.03 (24.63–50.78)
cFL [points lost per month] ⊠	0.95 ± 0.75 (0.11–4.02)

Abbreviations: ECAS Edinburgh Cognitive and Behavioral ALS Screen; FAB Frontal Assessment Battery; MMSE Mini-Mental State Exam; D50 overall disease aggressiveness; rD50 (relative D50) individual disease covered; cFS calculated Functional State; cFL calculated Functional Loss-rate.

Note: Continuous data are summarized for ⊠ as mean ± SD or for # as median ± interquartile range (each with the total range in brackets). For ⊕ categorical data, the number of cases (equals percentages) are given. Variables that are time point dependent refer to the day of MRI-acquisition; others depict constant characterization of patients' overall disease course.

decreases in GM volume in the left amygdala and left stratum of the hippocampus ($p < 0.05$ Holm-Bonferroni corrected, Fig. 1B). As in the CT-analyses, there were no significant increases in GM volume in any ROI for patients with ALS in comparison to HC.

3.3. Grey-matter alterations in relation to disease accumulation

Patients in Phase I (rD50 < 0.25) presented with higher CT in three different clusters compared to patients in higher phases. These clusters were in the inferolateral regions of bilateral precentral gyrus (PrCG) corresponding to facial and bulbar mototopic parts with an additional cluster in the right angular gyrus ($p < 0.001$; Fig. 2A). Adding age and gender as nuisance covariates to this phase comparison (in addition to type of onset and D50), still revealed the largest cluster in the right PrCG as significant ($p < 0.001$; indicated with a blue circle in Fig. 2A).

There were no significant increases in CT for patients in higher phases compared to patients in Phase I.

The subcortical ROI-analyses showed decreased GM volume in CA4 /dentate gyrus of the left hippocampus for patients in higher phases, while no subcortical volume increases were identified ($p < 0.05$ Holm-Bonferroni corrected, Fig. 2B).

Regression analyses revealed 20 clusters where decreased CT significantly correlated with higher rD50 ($p < 0.001$; Fig. 3A). These were located in bilateral occipital gyri, left inferolateral postcentral gyrus, right medial temporal gyrus, inferolateral PrCG, supramarginal gyrus and temporal pole. Adding age and gender as covariates in the model (in addition to the type of onset and D50) still resulted in three right-hemispheric significant clusters (right PrCG, right supramarginal

gyrus and right temporal pole). Regression analyses between subcortical GM volume and rD50 revealed negative correlations in bilateral thalamus, amygdala, Striatum and CA2_3, left inferior posterior cerebellum LVIIIA, CA4, stratum radiatum/ stratum lacunosum/stratum moleculare, and right inferior posterior cerebellum LX ($p < 0.05$ Holm-Bonferroni corrected, Fig. 3B).

No positive correlations were found for the parameter rD50, neither in CT- nor in ROI-analyses.

Another parameter describing the accumulated disease progression is the cFS (here also calculated for the time point of MRI). The regression analysis between cFS and CT identified 10 clusters with a positive correlation. Most of these clusters were alike with those clusters identified to show negative correlations between rD50 and CT. We revealed that CT of left inferolateral postcentral gyrus and parasagittal superior frontal gyrus, as well as right inferoprecentral sulcus and parasagittal occipital correlated positively with the cFS.

We observed positive correlations between cFS and GM volume in our predefined subcortical ROIs, namely bilateral thalamus, striatum, superior posterior cerebellum (LVIIB), left inferior posterior cerebellum (LX), and in right inferior posterior cerebellum (LVIIA). There were no significant negative correlations for cFS with neither CT nor ROI volumes.

3.4. Grey matter alterations in relation to disease aggressiveness

Both, CT- and ROI-analyses did not reveal any differences if comparing patients with higher disease aggressiveness (D50 > 30) to those with lower disease aggressiveness ($30 \leq D50$) or vice versa (at $p < 0.001$; Fig. 2C and 2D).

Likewise, our analyses did not find any significant correlations in regression analyses with the parameter D50 (neither for CT-, nor subcortical ROI-analyses).

3.5. Grey matter alterations in relation to cFL

There were neither positive nor negative correlations between CT and the cFL calculated for the timepoint of MRI. In subcortical ROI-analyses, a significant positive correlation between GM volume and cFL was revealed in the right thalamus ($p < 0.05$ Holm-Bonferroni corrected). Other ROIs showed neither positive nor negative correlations with the cFL.

4. Discussion

In this study we evaluated Cortical Thickness (CT) and subcortical GM volumes in the context of progressing ALS-pathology in a large cohort of well-characterized patients. We revealed several areas with significant cortical thinning and reductions of deep GM volumes in ALS patients as compared to HC (Fig. 1). Within the group of patients with ALS, we revealed that progressive decreases of CT and subcortical GM volume reductions correlate with accumulation of the ALS-disease. This was shown in subgroup-comparisons of patients in advanced phases with those in Phase I (Fig. 2); as well as in regression analyses with the parameters rD50 and cFS (Fig. 3). In contrast, measures of GM structural integrity were not associated with ALS disease aggressiveness, neither in subgroup, nor in direct regression analyses.

Our findings of widespread thinning of cortical GM in ALS patients (Fig. 1A) underscore pre-existing data reporting patterns of cortical atrophy in ALS (Agosta et al., 2012; Benbrika et al., 2021; Chen et al., 2018; Mezzapesa et al., 2013; Schuster et al., 2013; Verstraete et al., 2012). However, there are inconsistencies concerning findings, especially within the PrCG and some studies could not reveal any cortical thinning for the respective group of ALS patients (Cardenas-Blanco et al., 2016; Spinelli et al., 2020). We assume, that these differences can to a certain degree be attributed to the substantial heterogeneity in the ALS-populations investigated as well as methodological differences between

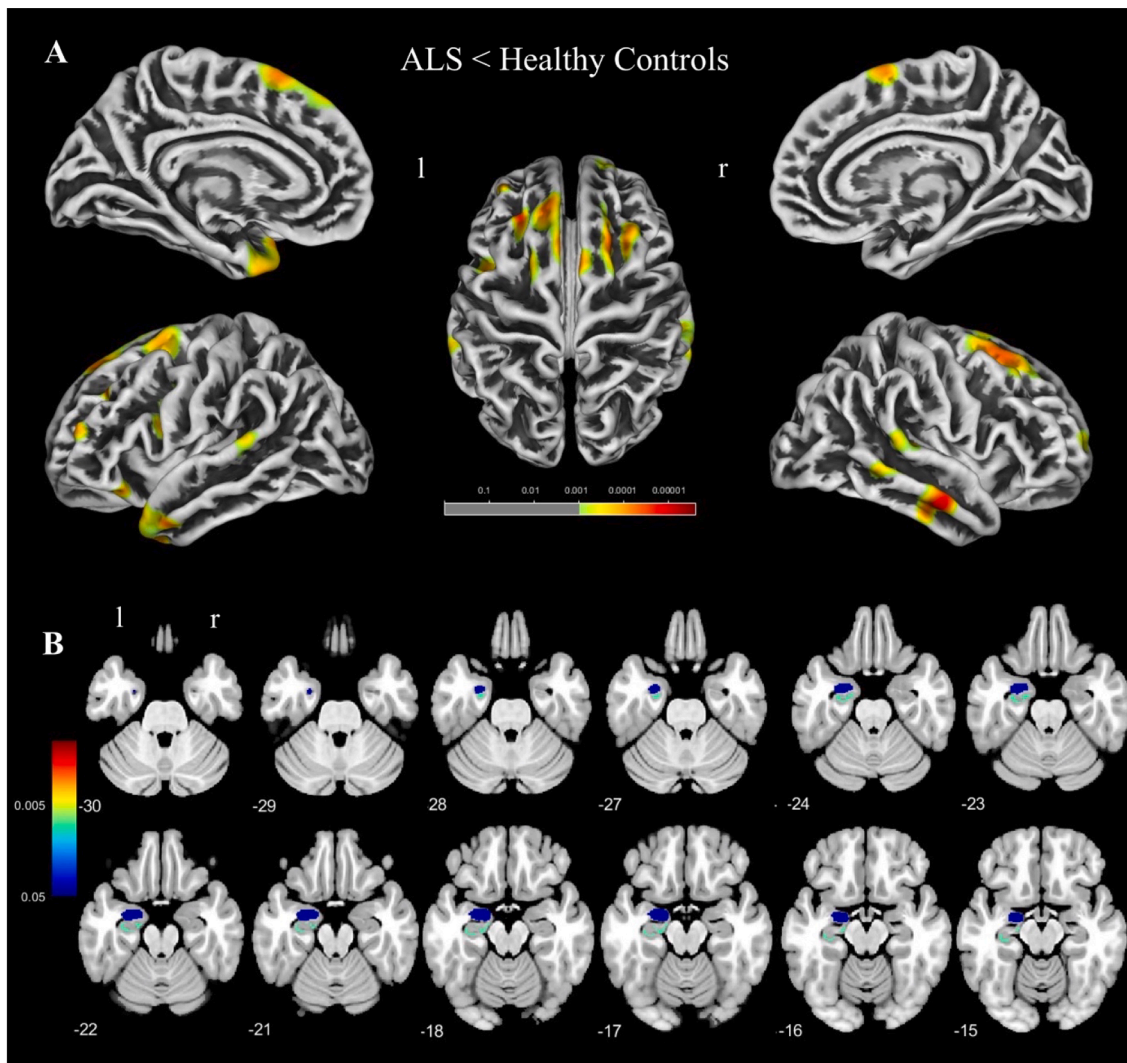


Fig. 1. Comparison of ALS-cohort with Healthy Controls.

a) Cross-sectional Cortical Thickness (CT)-analysis: A decrease in CT was observed mainly frontotemporal. Bilateral superior frontal gyrus, superior temporal gyrus, right medial temporal gyrus, and left temporal pole showed decreased CT in ALS-patients. ($p < 0.001$; cluster extent threshold at expected number of vertices per cluster, nuisance covariates: age, gender)

b) Cross-sectional ROI-analysis. Decrease of GM volume was significant in left-hemispheric amygdala and stratum of the hippocampus. ($p < 0.05$ Holm-Bonferroni corrected; nuisance covariates: age, gender, TIV)

Colorbars represent p -Values. *Abbreviations:* CT: Cortical Thickness; GM: Grey Matter; l: left hemisphere; r: right hemisphere; ROI: Region-Of-Interest; TIV: Total Intracranial Volume.

studies. More specifically, these may be differing degrees of ALS disease accumulation (Goyal et al., 2020; Spinelli et al., 2016), differing relations of bulbar and spinal involvement (Jin et al., 2018; Schuster et al., 2013; Steinbach et al., 2020), or the usage of 1.5T MRI-scans (Chu et al., 2017; Livshits et al., 2012; Sicotte et al., 2003), and the CAT12 algorithm (Seiger et al., 2018), just to name a few.

We observed decreased GM volumes in left amygdala and hippocampal ROIs in the case-control-comparison (Fig. 1B), which is in line with the existing literature (Finegan et al., 2020; Machts et al., 2015; van der Burgh et al., 2020; Westeneng et al., 2015). However, there are also discrepancies in the extent of subcortical structural involvement in ALS reported so far and some studies did not find any subcortical changes on a case-control level (Bede et al., 2018; Fu et al., 2021). Regarding the whole spectrum from pure-motoneuronal ALS to fronto-temporal dementia, previous studies suggest that selective vulnerability of subcortical grey-matter depends on the extend of cognitive and/or behavioural deficits, as well as the presence of ALS-causing genetic variants such as C9orf72 (Ahmed et al., 2021; Bede et al., 2018; Machts et al., 2015; van

der Burgh et al., 2020). Although the ALS patients of the study reported here had cognitive screening tests within normal ranges, subclinical deficiencies and especially behavioural impairment cannot be excluded and further studies are needed to decipher the underlying interplay of factors potentially influencing deep GM pathology. Altogether, our study supports and extends the existing evidence about widespread cortical and subcortical GM involvement in ALS in the sense of a multi-systemic neurodegenerative disease not being restricted to motoric areas.

Findings in our ALS-Subgroup comparisons and regression analyses revealed consistent correlations between CT and disease accumulation, independent of disease aggressiveness. Comparison of patients in different phases of disease (early stable Phase I versus higher phases) showed a systematic decrease of CT along with disease progression. Areas of lower CT associated with advanced disease phases were mainly located in bulbar parts of the PrCG, emphasized for the right hemisphere (Fig. 2A). This observation was additionally confirmed by regression analyses between individual rD50 and CT. With advanced disease

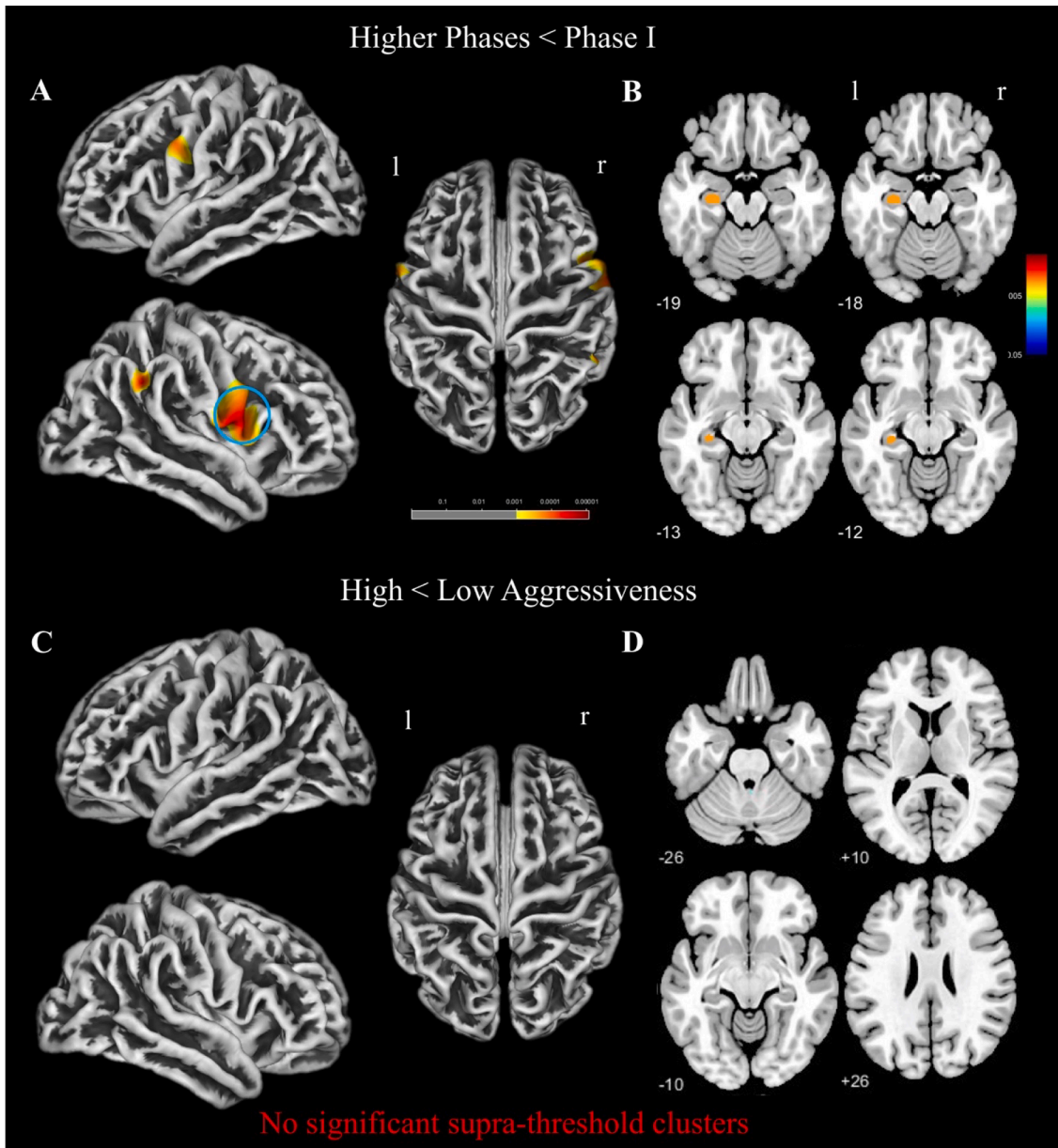


Fig. 2. Comparison of patients across disease phases.

a) Cortical Thickness (CT) subgroup-analysis of patients in disease Phase I ($rd50 < 0.25$, $n = 48$) versus higher phases ($rd50 \geq 0.25$, $n = 52$) at the time of MRI acquisition: Decrease in CT in higher phases were observed in the bilateral inferolateral precentral gyrus and the right angular gyrus in contrast to Phase I. ($p < 0.001$; cluster extent threshold at expected number of voxels per cluster; nuisance covariates: type of onset, D50). Blue circles represent clusters remaining significant after adding age and gender as nuisance covariates.

b) Subgroup ROI-analysis between patients in Phase I and higher phases at the time of MRI acquisition: Decrease in GM volume was identified in the CA4 of hippocampus ($p < 0.05$ Holm-Bonferroni corrected; nuisance covariates: type of onset, D50, TIV)

There were no significant increases of CT or GM volume across disease phases.

Comparison across disease aggressiveness subgroups

c) CT subgroup analysis of patients with high ($D50 < 30$ months, $n = 49$) versus low ($D50 \geq 30$ months, $n = 51$) overall disease aggressiveness revealed no CT increases or decreases. ($p < 0.001$; cluster extent threshold at expected number of vertices per cluster; nuisance covariates: type of onset, $rd50$)

d) Subgroup ROI-analysis also revealed no significant differences between subgroups. ($p < 0.05$ Holm-Bonferroni corrected; nuisance covariates: type of onset, $rd50$, TIV)

Colorbars represent p -Values. *Abbreviations:* CT: Cortical Thickness; GM: Grey Matter; l: left hemisphere; r: right hemisphere; ROI: Region-Of-Interest; TIV: Total Intracranial Volume.

covered (higher $rd50$), CT significantly decreased in right precentral sulcus, temporal pole, and supramarginal gyrus. Altogether, this suggests that declining CT is an ongoing process whilst the ALS disease progresses. There are previous studies aiming at finding associations between clinical disease progression and measures of structural GM integrity, however reporting controversial results. Some authors did not

find any alterations in CT in the course of the disease (Cardenas-Blanco et al., 2016; de Albuquerque et al., 2017; Spinelli et al., 2020). In contrast, other longitudinal studies were able to identify specific regions with progressive decline of GM volume or CT over time (Bede and Hardiman, 2018; Benbrika et al., 2021; Kwan et al., 2012; van der Burgh et al., 2020). However, whilst some other studies found longitudinal

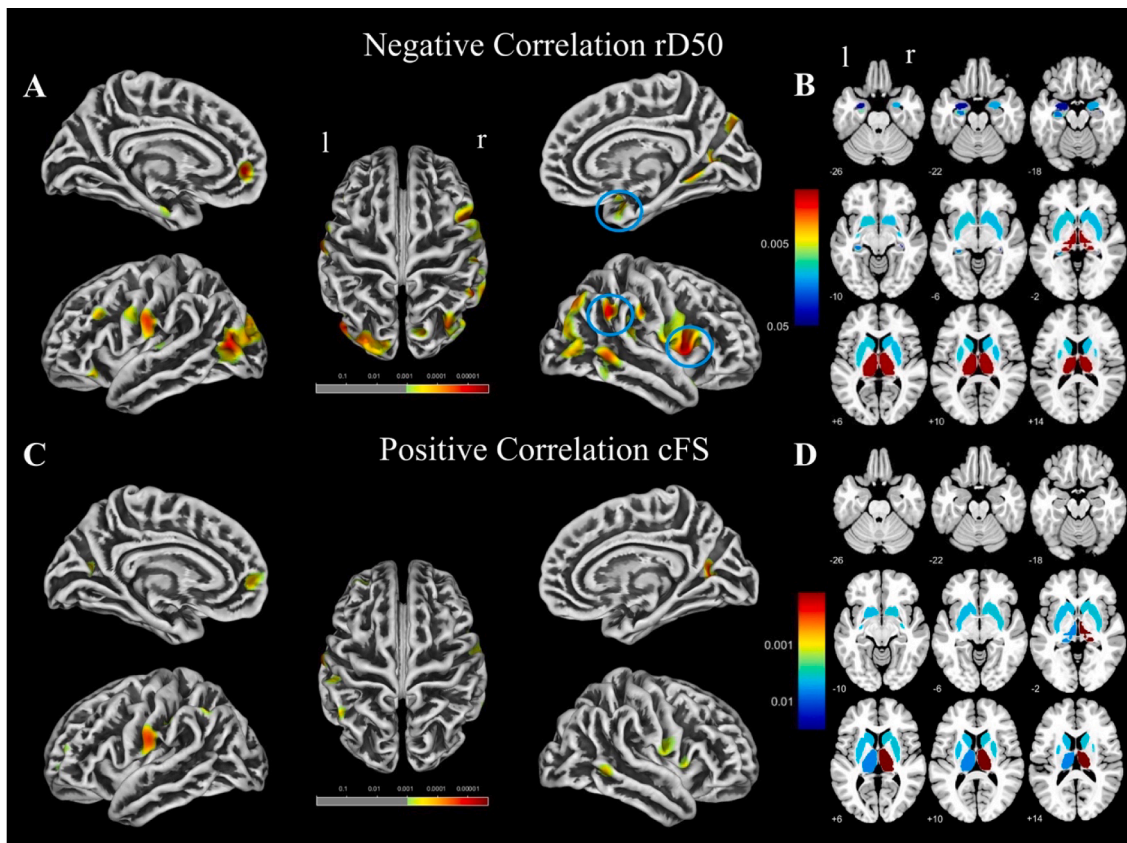


Fig. 3. Multiple Regression analyses with rD50.

a) CT decreases were inversely correlated with rD50 (with increasing disease covered) in bilateral inferolateral pre-, and postcentral sulcus, bilateral occipital gyri, and multiple frontal and temporal clusters. ($p < 0.001$; cluster extent threshold at expected number of vertices per cluster; nuisance covariates: type of onset, D50). Blue circles represent cluster remaining significant after adding age and gender as nuisance covariates.

b) In subcortical ROI decrease of GM volume with increase of rD50 was identified in the bilateral thalamus, amygdala, Striatum and CA2_3, the left inferior posterior cerebellum LVIIIA, CA4, stratum and the right inferior posterior cerebellum LX. ($p < 0.05$ Holm-Bonferroni corrected; nuisance covariates: type of onset, D50, TIV) Multiple Regression analyses with cFS

c) Positive correlations between cFS and CT were revealed in the bilateral inferolateral pre-, and postcentral gyrus, occipital gyri, right medial temporal and supramarginal gyrus and in smaller clusters in the frontal cortex. ($p < 0.001$; cluster extent threshold at expected number of vertices per cluster; nuisance covariates: type of onset, cFL)

d) Increase of GM volume along with increase of cFS was significant in the bilateral thalamus, striatum, superior posterior LVIIB cerebellum, the left inferior posterior cerebellum LX and in the right inferior posterior cerebellum LVIA. ($p < 0.05$ Holm-Bonferroni corrected; nuisance covariates: type of onset, cFL, TIV) There were no significant positive correlations with rD50 or negative correlations with cFS observable.

Colorbars represent p -Values. Abbreviations: cFS: calculated Functional State; cFL: calculated Functional Loss-Rate; CT: Cortical Thickness; GM: Grey Matter; l: left hemisphere; r: right hemisphere; ROI: Region-Of-Interest; TIV: Total Intracranial Volume.

decreases of CT in GM regions, they were not able to correlate them to the decline of clinical disabilities as measured by the ALSFRS-R (de Albuquerque et al., 2017; Schuster et al., 2014). Another group investigating C9orf72 variant carriers found a weak correlation between longitudinal ALSFRS-R changes and the CT of bilateral PrCG but not for other cortical regions (Floeter et al., 2016).

The correlations between parameters of disease accumulation (i.e., rD50 and cFS) and CT-decreases reported in this study therefore again highlight the advantages of using the D50-model instead of the original ALSFRS-R scores susceptible to (intra- and inter-)rater-variability (Bakker et al., 2020; Steinbach et al., 2021a). A pitfall of longitudinal studies in ALS and therefore another advantage of the D50-model arises from the usage of fixed time-intervals in between MRI-scans. This leads to known difficulties in recruitment and sampling-bias due to the naturally high drop-out rates in ALS cohorts (e.g., poor longevity or inability to lie in a MRI scanner). The remaining patients in longitudinal MRI studies are often those with lower disease aggressiveness, longer survival, more spinal onset, and younger age at onset (de Albuquerque et al., 2017; van der Burgh et al., 2020). Therefore, results cannot

reliably represent the ALS-population as a whole or lack effect size (de Albuquerque et al., 2017; Spinelli et al., 2020). We already suggested the possibility that the D50-model can approximate longitudinal results from a cross-sectional data set in a former study (Prell et al., 2020). Thus, we were able to principally circumvent restrictions of longitudinal studies, because the D50-model allows quantification of patients' individual disease course.

Here, we could examine relations between the loss of brain structure and the amount of clinical disease covered (rD50), independent of disease aggressiveness (corrected for D50). As such, found correlations represent progressive loss of GM structural integrity that are directly correlated with clinical disability-related functional impairment caused by the progressing ALS disease. This observation was further substantiated by the significant correlations between the cFS and CT in areas mainly overlapping with those significant in the regression between rD50 and CT. This is of note since cFS describes the local remaining rest- functionality for daily live abilities of a patient, here calculated for the time point of MRI, and is therefore the parameter that corresponds the most closely to the traditional ALSFRS-R value.

Altogether, we are confident to conclude that decreasing CT is a reliable biomarker reflecting progressive neurodegeneration in ALS, related to worsening of clinical disability. Further, the possible use of CT as a marker of disease progression is supported by the observation, that no inverse association could be found. Indeed, there was no increased GM in patients at advanced disease phases, and accordingly neither positive correlations with rD50 nor negative correlations with cFS could be revealed. Hence, our data support the notion that atrophy of GM during the clinical course of the ALS disease is a constant, one-directional process.

Few studies so far examined potential associations between subcortical alterations and disease parameters of ALS disease progression. In a longitudinal analysis of subcortical GM in ALS, enlargement of ventricles and decreased GM volumes in hippocampal subfields were found in follow-up MRI but no significant longitudinal alterations in thalamus, caudatus, putamen, pallidum, hippocampus, amygdala or accumbens (Westeneng et al., 2015).

Menke et al. (2014) reported a longitudinal GM decline in subcortical areas, but they were not able to correlate clinical disability (ALSFRS-R total score) with GM integrity using VBM, neither in whole-brain nor in ROI-based analyses.

However, in our study we observed that loss of GM in subcortical regions is also associated with parameters of disease accumulation, similar to our CT-analyses. Subgroup comparison between patients in Phase I and higher phases showed a decline of GM volume limited to CA4/DG of the left hippocampus. In regression analyses with the parameter rD50, decreasing subcortical volumes could also be revealed in bilateral thalamus, amygdala, striatum, different regions in right and left hippocampus and areas in inferior posterior cerebellum – all these regions showing negative correlation between GM volume and rD50. Further, regression with cFS showed matching results with a positive correlation significant in mostly similar regions. Especially decreases in hippocampal subfields and thalamus along the progressing disease is in good accordance with previous findings of studies using longitudinal models in their research (Menke et al., 2014; Westeneng et al., 2015).

In this study we used a ROI-based approach for analyses in subcortical structures and were able to show consistent associations between subcortical decline of GM volume and clinical measures of disease accumulation. Our results regarding subcortical ROIs reflect, that ongoing atrophy of GM is not restricted to cortical structures but can equally be detected in hippocampal regions, thalamus, basal ganglia, and the cerebellum.

In contrast to the observed associations with parameters of disease accumulation, we could not find any relations between GM atrophy and disease aggressiveness. This was the case for subgroup-comparison of patients subdivided according to their individual D50-value as well as in direct regression analyses with the parameter D50. This underlines our prior observations that structural integrity of GM in ALS is independent of disease aggressiveness, using a whole-brain-based approach with VBM (Steinbach et al., 2020).

So far, some former studies used the Progression Rate (PR) as a parameter for disease progression-speed in ALS, calculated as the linear ALSFRS-R decline over time $((48 - \text{ALSFRS-R}) / \text{disease duration})$. Using the PR, Menke et al. (2014) did not identify associations between PR and GM measures, which is in accordance with our findings. In another approach, studies examined associations between discovered longitudinal changes in neuroimaging measures of grey matter structures and the local, linearly approximated decline of the ALSFRS-R score over time, i.e. the ALSFRS-R slope. This also revealed inconsistent results in former studies: de Albuquerque et al. (2017) did not find any correlations between observed reductions of brainstem GM volume and clinical scores including the ALSFRS-R slope, but (Kwan et al., 2012) reported correlations between the decline of the ALSFRS-R score and loss of precentral GM volume. However, due to the known curvilinear decline of ALSFRS-R points over time, slopes calculated based on the ALSFRS-R score differ depending on defined time points used to calculate the

ALSFRS-R slope (Gordon et al., 2010; Senda et al., 2017). The data of the study reported here strongly supports that disease aggressiveness in ALS does not influence the degree of structural loss in GM. In contrast, several previous studies underscore that WM rather than GM alterations are driving disease aggressiveness in ALS (Steinbach et al., 2021a). Our recent findings in this new work are now able to accentuate the likely independence between GM and disease aggressiveness. We could extend knowledge about missing associations between GM atrophy and disease aggressiveness onto the biomarker cortical thickness, described as having better accuracy than VBM-measures (Desai et al., 2005) and further to subcortical atrophy patterns.

Regarding the high associations between GM atrophy and parameters of disease accumulation (rD50 and cFS) after correcting for background disease activity and connecting those findings to the noticeable results that there are no correlations with disease aggressiveness (D50), it is reasonable to conclude that alterations in GM are robust markers of disease accumulation, independent of disease aggressiveness.

Our study has some limitations. Our data is monocentric, including only patients from one tertiary ALS center and validation of the neuroimaging results in independent cohorts is necessary. Moreover, the data cannot be generalized for the entire ALS population because of potential referral bias. Patients in tertiary ALS centers are often younger (thus having longer survival times) and show a relatively smaller proportion of bulbar-onset patients (Logroscino et al., 2018; Sorenson et al., 2007). In our study, the patients in higher phases of ALS were significantly older than those in Phase I. However, the D50-model allows better comparability of different patients and provides the ability to calculate parameters that represent the course of the disease as a whole for every given time point. This allowed us to perform a pseudolongitudinal study of the entire cohort of ALS patients in this MRI study. However, verification through real longitudinal data is desirable but naturally will depend on large, well-designed multi-center studies (Kalra et al., 2020; Steinbach et al., 2018). Besides, our patients were only assessed via neuropsychological screening tests and therefore subclinical cognitive deficits and/or behavioral impairment are possible. Further, genetic testing was not available for all patients, and we could not characterize or exclude patients based on genetic profiles. A statistical limitation of our study is that CT results are reported with a cluster extent threshold to minimize the probability of an inflation of Type I error, however a lower spatial specificity in larger clusters has to be taken into account if using this method. Future studies using a higher MRI field strength (e.g., 3T) are also needed to see, if this would influence the neuroimaging results, as would be methodological comparison studies (e.g., using FreeSurfer).

5. Conclusion

In this study, we analyzed cortical thickness and subcortical grey matter in relation to ALS disease progression. By application of the D50 model, we were able to examine associations of those neuroimaging markers with disease accumulation independent of disease aggressiveness and vice versa. This allowed quantification and comparability of the heterogeneous disease course of the patients with ALS and a well-defined big cohort could be included representing the population referred to our tertiary center. Thus, we were able to identify correlations between loss of grey matter structure, cortical and subcortical, and disease accumulation. Most important, independence of grey matter structural integrity was confirmed in relation to disease aggressiveness. Altogether, this highly qualifies the neuroimaging measures used in this study to be applicable as biomarkers of pure disease accumulation, independent of the background activity of disease. This is most relevant for upcoming clinical trials as well as clinical management in ALS since the success of therapeutic interventions relies on biomarkers robustly quantifying disease covered/accumulation.

CRedit authorship contribution statement

Nora Dieckmann: Software, Formal analysis, Investigation, Writing – original draft, Writing – review & editing, Visualization. **Annekathrin Roediger:** Investigation, Writing – review & editing. **Tino Prell:** Formal analysis, Writing – review & editing. **Simon Schuster:** Data curation, Writing – review & editing. **Meret Herdick:** Data curation, Writing – review & editing. **Thomas E. Mayer:** Investigation, Resources, Writing – review & editing. **Otto W. Witte:** Writing – review & editing, Funding acquisition. **Robert Steinbach:** Conceptualization, Methodology, Software, Validation, Investigation, Resources, Data curation, Writing – original draft, Writing – review & editing, Visualization, Funding acquisition. **Julian Grosskreutz:** Conceptualization, Methodology, Investigation, Resources, Data curation, Writing – review & editing, Supervision, Project administration, Funding acquisition.

Declaration of Competing Interest

The authors declare that they have no known competing financial interests or personal relationships that could have appeared to influence the work reported in this paper.

Acknowledgments

We are grateful to the community of ALS patients and their caregivers, without whom this work would not be possible. We extend our thanks to Mandy Arnold, Annkathrin Klose, and Cindy Hoepfner for continuous assessment and patient care.

Funding

The present study was supported by the German Bundesministerium für Bildung und Forschung (BMBF) grant SOPHIA [01ED1202B] and ONWebDUALS [01ED15511A] to JG under the aegis of the EU Joint Program Neurodegenerative Disease Research (JPND) and a BMBF grant PYRAMID [01GM1304] to JG in the framework of the ERANET E-RARE program. Support was also received from the Motor Neurone Disease Association (MNDA) and Deutsche Gesellschaft fuer Muskelkranke (DGM). ND is supported by funding from the foundation “Else-Kröner-Fresenius-Stiftung” within the Else Kröner Graduate School for Medical Students “Jena School for Ageing Medicine (JSAM)”. RS and AR are supported by the Deutsche Forschungsgemeinschaft (DFG) with a clinician scientist program [413668513]. Funding was also provided by the Interdisciplinary Center of Clinical Research of the Medical Faculty Jena.

Appendix A. Supplementary data

Supplementary data to this article can be found online at <https://doi.org/10.1016/j.nicl.2022.103162>.

References

- Abrahams, S., Newton, J., Niven, E., Foley, J., Bak, T.H., 2014. Screening for cognition and behaviour changes in ALS. *Amyotroph. Lateral Scler. Frontotemporal. Degener.* 15 (1-2), 9–14.
- Agosta, F., Pagani, E., Rocca, M.A., Caputo, D., Perini, M., Salvi, F., Prella, A., Filippi, M., 2007. Voxel-based morphometry study of brain volumetry and diffusivity in amyotrophic lateral sclerosis patients with mild disability. *Hum. Brain Mapp.* 28 (12), 1430–1438.
- Agosta, F., Valsasina, P., Riva, N., Copetti, M., Messina, M.J., Prella, A., Comi, G., Filippi, M., Le, W., 2012. The cortical signature of amyotrophic lateral sclerosis. *PLoS ONE* 7 (8), e42816.
- Ahmed, R.M., Bocchetta, M., Todd, E.G., Tse, N.Y., Devenney, E.M., Tu, S., Caga, J., Hodges, J.R., Halliday, G.M., Irish, M., Kiernan, M.C., Piguet, O., Rohrer, J.D., 2021. Tackling clinical heterogeneity across the amyotrophic lateral sclerosis-frontotemporal dementia spectrum using a transdiagnostic approach. *Brain Commun.* 3, fcab257.
- Anticevic, A., Dierker, D.L., Gillespie, S.K., Repovs, G., Csernansky, J.G., Van Essen, D.C., Barch, D.M., 2008. Comparing surface-based and volume-based analyses of functional neuroimaging data in patients with schizophrenia. *Neuroimage* 41 (3), 835–848.
- Appollonio, I., Leone, M., Isella, V., Piamarta, F., Consoli, T., Villa, M.L., Forapani, E., Russo, A., Nichelli, P., 2005. The Frontal Assessment Battery (FAB): normative values in an Italian population sample. *Neurol. Sci.* 26 (2), 108–116.
- Ashburner, J., Friston, K.J., 2000. Voxel-based morphometry—the methods. *Neuroimage* 11 (6), 805–821.
- Bakker, L.A., Schröder, C.D., Tan, H.H.G., Vugts, S.M.A.G., van Eijk, R.P.A., van Es, M.A., Visser-Meily, J.M.A., van den Berg, L.H., 2020. Development and assessment of the inter-rater and intra-rater reproducibility of a self-administration version of the ALSFRS-R. *J. Neurol. Neurosurg. Psychiatry* 91 (1), 75–81.
- Bede, P., Hardiman, O., 2018. Longitudinal structural changes in ALS: a three time-point imaging study of white and gray matter degeneration. *Amyotroph. Lateral Scler. Frontotemporal. Degener.* 19 (3-4), 232–241.
- Bede, P., Elamin, M., Byrne, S., McLaughlin, R.L., Kenna, K., Vajda, A., Pender, N., Bradley, D.G., Hardiman, O., 2013. Basal ganglia involvement in amyotrophic lateral sclerosis. *Neurology* 81 (24), 2107–2115.
- Bede, P., Omer, T., Finegan, E., Chipika, R.H., Iyer, P.M., Doherty, M.A., Vajda, A., Pender, N., McLaughlin, R.L., Hutchinson, S., Hardiman, O., 2018. Connectivity-based characterisation of subcortical grey matter pathology in frontotemporal dementia and ALS: a multimodal neuroimaging study. *Brain Imaging Behav.* 12 (6), 1696–1707.
- Benbrika, S., Doidy, F., Carlier, L., Mondou, A., Pelerin, A., Eustache, F., Viader, F., Desgranges, B., 2021. Longitudinal Study of Cognitive and Emotional Alterations in Amyotrophic Lateral Sclerosis: Clinical and Imaging Data. *Front. Neurol.* 12, 620198.
- Brooks, B.R., Miller, R.G., Swash, M., Munsat, T.L., 2000. El Escorial revisited: revised criteria for the diagnosis of amyotrophic lateral sclerosis. *Amyotroph. Lateral Scler. Other Motor Neuron Disord.* 1 (5), 293–299.
- Cardenas-Blanco, A., Machts, J., Acosta-Cabrero, J., Kaufmann, J., Abdulla, S., Kollwe, K., Petri, S., Schreiber, S., Heinze, H.J., Dengler, R., Vielhaber, S., Nestor, P. J., 2016. Structural and diffusion imaging versus clinical assessment to monitor amyotrophic lateral sclerosis. *Neuroimage Clin.* 11, 408–414.
- Chen, Z.Y., Liu, M.Q., Ma, L., 2018. Cortical thinning pattern of bulbar- and spinal-onset amyotrophic lateral sclerosis: a surface-based morphometry study. *Chin. Med. Sci. J.* 33, 100–106.
- Chu, R., Hurwitz, S., Tauhid, S., Bakshi, R., 2017. Automated segmentation of cerebral deep gray matter from MRI scans: effect of field strength on sensitivity and reliability. *BMC Neurol.* 17, 172.
- Creavin, S.T., Wisniewski, S., Noel-Storr, A.H., Trevelyan, C.M., Hampton, T., Rayment, D., Thom, V.M., Nash, K.J., Elhamoui, H., Milligan, R., Patel, A.S., Tsvitos, D.V., Wing, T., Phillips, E., Kellman, S.M., Shackleton, H.L., Singleton, G.F., Neale, B.E., Watton, M.E., Cullum, S., 2016. Mini-Mental State Examination (MMSE) for the detection of dementia in clinically unevaluated people aged 65 and over in community and primary care populations. *Cochrane Database Syst Rev*, CD011145.
- Dahnke, R., Yotter, R.A., Gaser, C., 2013. Cortical thickness and central surface estimation. *Neuroimage* 65, 336–348.
- d’Ambrosio, A., Gallo, A., Trojsi, F., Corbo, D., Esposito, F., Cirillo, M., Monsurro, M.R., Tedeschi, G., 2014. Frontotemporal cortical thinning in amyotrophic lateral sclerosis. *AJNR Am. J. Neuroradiol.* 35 (2), 304–310.
- de Albuquerque, M., Branco, L.M., Rezende, T.J., de Andrade, H.M., Nucci, A., Franca Jr., M.C., 2017. Longitudinal evaluation of cerebral and spinal cord damage in Amyotrophic Lateral Sclerosis. *Neuroimage Clin.* 14, 269–276.
- Desai, R., Lieberthal, E., Possing, E.T., Waldron, E., Binder, J.R., 2005. Volumetric vs. surface-based alignment for localization of auditory cortex activation. *Neuroimage* 26 (4), 1019–1029.
- Dreger, M., Steinbach, R., Gaur, N., Metzner, K., Stubendorff, B., Witte, O.W., Grosskreutz, J., 2021. Cerebrospinal fluid neurofilament light chain (NfL) predicts disease aggressiveness in amyotrophic lateral sclerosis: An application of the D50 disease progression model. *Front. Neurosci.* 15, 651651.
- Dubois, B., Slachevsky, A., Litvan, I., Pillon, B., 2000. The FAB: a Frontal Assessment Battery at bedside. *Neurology* 55 (11), 1621–1626.
- Entis, J.J., Doerga, P., Barrett, L.F., Dickerson, B.C., 2012. A reliable protocol for the manual segmentation of the human amygdala and its subregions using ultra-high resolution MRI. *Neuroimage* 60 (2), 1226–1235.
- Finegan, E., Hi Shing, S.L., Chipika, R.H., McKenna, M.C., Doherty, M.A., Hengeveld, J. C., Vajda, A., Donaghy, C., McLaughlin, R.L., Hutchinson, S., Hardiman, O., Bede, P., 2020. Thalamic, hippocampal and basal ganglia pathology in primary lateral sclerosis and amyotrophic lateral sclerosis: Evidence from quantitative imaging data. *Data Brief* 29, 105115.
- Floeter, M.K., Bageac, D., Danielian, L.E., Braun, L.E., Traynor, B.J., Kwan, J.Y., 2016. Longitudinal imaging in C9orf72 mutation carriers: Relationship to phenotype. *Neuroimage Clin.* 12, 1035–1043.
- Frangou, S., Modabbernia, A., Williams, S.C.R., Papachristou, E., Doucet, G.E., Agartz, I., Aghajani, M., Akudjedu, T.N., Albajes-Eizaguirre, A., Alnaes, D., Alpert, K.L., Andersson, M., Andreasen, N.C., Andreasen, O.A., Asherson, P., Banaschewski, T., Bargallo, N., Baumeister, S., Baur-Streubel, R., Bertolino, A., Bonvino, A., Boomsma, D.I., Borgwardt, S., Bourque, J., Brandeis, D., Breier, A., Brodaty, H., Brouwer, R.M., Buitelaar, J.K., Busatto, G.F., Buckner, R.L., Calhoun, V., Canales-Rodriguez, E.J., Cannon, D.M., Caseras, X., Castellanos, F.X., Cervenka, S., Chaim-Avancini, T.M., Ching, C.R.K., Chubbar, V., Clark, V.P., Conrod, P., Conzelmann, A., Crespo-Facorro, B., Crivello, F., Crone, E.A., Dale, A.M., Dannlowski, U., Davey, C., de Geus, E.J.C., de Haan, L., de Zubicaraj, G.I., den Braber, A., Dickie, E.W., Di Giorgio, A., Doan, N.T., Dorum, E.S., Ehrlich, S., Erk, S., Espeseth, T., Fatouros-Bergman, H., Fisher, S.E., Fouche, J.P., Franke, B., Frodl, T., Fuentes-Claramonte, P., Glahn, D.C., Gotlib, I.H., Grabe, H.J., Grimm, O., Groenewold, N.A., Grotegerd, D.,

- Gruber, O., Gruner, P., Gur, R.E., Gur, R.C., Hahn, T., Harrison, B.J., Hartman, C.A., Hatton, S.N., Heinz, A., Heslenfeld, D.J., Hibar, D.P., Hickie, I.B., Ho, B.C., Hoeskstra, P.J., Hohmann, S., Holmes, A.J., Hoogman, M., Hosten, N., Howells, F.M., Hulshoff Pol, H.E., Huysler, C., Jahanshad, N., James, A., Jernigan, T.L., Jiang, J., Jonsson, E.G., Joska, J.A., Kahn, R., Kalnin, A., Kanai, R., Klein, M., Klyushnik, T.P., Koenders, L., Koops, S., Kramer, B., Kuntsi, J., Lagopoulos, J., Lazaro, L., Lebedeva, I., Lee, W.H., Lesch, K.P., Lochner, C., Machielsen, M.W.J., Maingault, S., Martin, N.G., Martinez-Zalacain, I., Mataix-Cols, D., Mazoyer, B., McDonald, C., McDonald, B.C., McIntosh, A.M., McMahon, K.L., McPhilemy, G., Meinert, S., Menchon, J.M., Medland, S.E., Meyer-Lindenberg, A., Naaijen, J., Najt, P., Nakao, T., Nordvik, J.E., Nyberg, L., Oosterlaan, J., de la Foz, V.O., Paloyelis, Y., Pauli, P., Pergola, G., Pomarol-Clotet, E., Portella, M.J., Potkin, S.G., Radua, J., Reif, A., Rinker, D.A., Roffman, J.L., Rosa, P.G.P., Sacchet, M.D., Sachdev, P.S., Salvador, R., Sanchez-Juan, P., Sarro, S., Satterthwaite, T.D., Saykin, A.J., Serpa, M.H., Schmaal, L., Schnell, K., Schumann, G., Sim, K., Smoller, J.W., Sommer, I., Soriano-Mas, C., Stein, D.J., Strike, L.T., Swagerman, S.C., Tamnes, C.K., Temmingh, H.S., Thomopoulos, S.I., Tomyshv, A.S., Tordesillas-Gutierrez, D., Trollor, J.N., Turner, J. A., Uhlmann, A., van den Heuvel, O.A., van den Meer, D., van der Wee, N.J.A., van Haren, N.E.M.D., van 't Ent, van Erp, T.G.M., Veer, I.M., Veltman, D.J., Voineskos, A., Volzke, H., Walter, H., Walton, E., Wang, L., Wang, Y., Wassink, T.H., Weber, B., Wen, W., West, J.D., Westlye, L.T., Whalley, H., Wierenga, L.M., Wittfeld, K., Wolf, D.H., Worker, A., Wright, M.J., Yang, K., Yoncheva, Y., Zanetti, M. V., Ziegler, G.C., Karolinska Schizophrenia, P., Thompson, P.M., Dima, D., 2022. Cortical thickness across the lifespan: Data from 17,075 healthy individuals aged 3–90 years. *Hum. Brain Mapp.* 43, 431–451.
- Fu, T., Kobleva, X., Bronzlik, P., Nösel, P., Dadak, M., Lanfermann, H., Petri, S., Ding, X.-Q., 2021. Clinically applicable quantitative magnetic resonance morphologic measurements of grey matter changes in the human brain. *Brain Sci.* 11 (1), 55.
- Gordon, P.H., Cheng, B., Salachas, F., Pradat, P.-F., Bruneteau, G., Corcia, P., Lacomblez, L., Meininger, V., 2010. Progression in ALS is not linear but is curvilinear. *J. Neurol.* 257 (10), 1713–1717.
- Goyal, N.A., Berry, J.D., Windebank, A., Staff, N.P., Maragakis, N.J., Berg, L.H., Genge, A., Miller, R., Baloh, R.H., Kern, R., Gothelf, Y., Lebovits, C., Cudkovic, M., 2020. Addressing heterogeneity in amyotrophic lateral sclerosis CLINICAL TRIALS. *Muscle Nerve* 62 (2), 156–166.
- Jiao, Y., Chen, R., Ke, X., Chu, K., Lu, Z., Herskovits, E.H., 2010. Predictive models of autism spectrum disorder based on brain regional cortical thickness. *Neuroimage* 50 (2), 589–599.
- Jin, K., Zhang, T., Shaw, M., Sachdev, P., Cherbuin, N., 2018. Relationship between sulcal characteristics and brain aging. *Front. Aging Neurosci.* 10, 339.
- Kalra, S., Müller, H.-P., Ishaque, A., Zinman, L., Korngut, L., Genge, A., Beaulieu, C., Frayne, R., Graham, S.J., Kassubek, J., 2020. A prospective harmonized multicenter DTI study of cerebral white matter degeneration in ALS. *Neurology* 95 (8), e943–e952.
- Kiernan, M.C., Vucic, S., Cheah, B.C., Turner, M.R., Eisen, A., Hardiman, O., Burrell, J.R., Zoing, M.C., 2011. Amyotrophic lateral sclerosis. *Lancet* 377 (9769), 942–955.
- Kiernan, M.C., Vucic, S., Talbot, K., McDermott, C.J., Hardiman, O., Shefner, J.M., Al-Chalabi, A., Huynh, W., Cudkovic, M., Talman, P., Van den Berg, L.H., Dharmadasa, T., Wicks, P., Reilly, C., Turner, M.R., 2021. Improving clinical trial outcomes in amyotrophic lateral sclerosis. *Nat Rev Neurol* 17 (2), 104–118.
- Kwan, J.Y., Meoded, A., Danielian, L.E., Wu, T., Floeter, M.K., 2012. Structural imaging differences and longitudinal changes in primary lateral sclerosis and amyotrophic lateral sclerosis. *Neuroimage Clin* 2, 151–160.
- Livshits, I., Hussein, S., Kennedy, C., Weinstein-Guttman, B., Hohnacki, D., Zivadinov, R., 2012. Comparison of a 1.5T standard vs. 3T optimized protocols in multiple sclerosis patients. *Minerva Med.* 103, 97–102.
- Logrosino, G., Marin, B., Piccininni, M., Arcuti, S., Chiò, A., Hardiman, O., Rooney, J., Zoccollella, S., Couratier, P., Preux, P.-M., Beghi, E., Fasano, A., 2018. Referral bias in ALS epidemiological studies. *PLoS ONE* 13 (4), e0195821.
- Longinetti, E., Fang, F., 2019. Epidemiology of amyotrophic lateral sclerosis: an update of recent literature. *Curr. Opin. Neurol.* 32, 771–776.
- Lule, D., Burkhardt, C., Abdulla, S., Böhm, S., Kollwe, K., Uttner, I., Abrahams, S., Bak, T.H., Petri, S., Weber, M., Ludolph, A.C., 2015. The Edinburgh Cognitive and Behavioural Amyotrophic Lateral Sclerosis Screen: a cross-sectional comparison of established screening tools in a German-Swiss population. *Amyotroph. Lateral Scler. Frontotemporal Degener.* 16 (1–2), 16–23.
- Machts, J., Loewe, K., Kaufmann, J., Jakubiczka, S., Abdulla, S., Petri, S., Dengler, R., Heinze, H.-J., Vielhaber, S., Schoenfeld, M.A., Bede, P., 2015. Basal ganglia pathology in ALS is associated with neuropsychological deficits. *Neurology* 85 (15), 1301–1309.
- Magen, I., Yacovzada, N.S., Yanowski, E., Coenen-Stass, A., Grosskreutz, J., Lu, C.-H., Greensmith, L., Malaspina, A., Fratta, P., Hornstein, E., 2021. Circulating miR-181 is a prognostic biomarker for amyotrophic lateral sclerosis. *Nat. Neurosci.* 24 (11), 1534–1541.
- Menke, R.A., Komer, S., Filippini, N., Douaud, G., Knight, S., Talbot, K., Turner, M.R., 2014. Widespread grey matter pathology dominates the longitudinal cerebral MRI and clinical landscape of amyotrophic lateral sclerosis. *Brain* 137, 2546–2555.
- Mezzapesa, D.M., D'Errico, E., Tortelli, R., Distaso, E., Cortese, R., Tursi, M., Federico, F., Zoccollella, S., Logrosino, G., Dicuozzo, F., Simone, I.L., Pirko, I., 2013. Cortical thinning and clinical heterogeneity in amyotrophic lateral sclerosis. *PLoS ONE* 8 (11), e80748.
- Park, M.T., Pipitone, J., Baer, L.H., Winterburn, J.L., Shah, Y., Chavez, S., Schira, M.M., Lobaugh, N.J., Lerch, J.P., Voineskos, A.N., Chakravarty, M.M., 2014. Derivation of high-resolution MRI atlases of the human cerebellum at 3T and segmentation using multiple automatically generated templates. *Neuroimage* 95, 217–231.
- Pereira, J.B., Ibarretxe-Bilbao, N., Marti, M.-J., Compta, Y., Junqué, C., Bargallo, N., Tolosa, E., 2012. Assessment of cortical degeneration in patients with Parkinson's disease by voxel-based morphometry, cortical folding, and cortical thickness. *Hum. Brain Mapp.* 33 (11), 2521–2534.
- Prell, T., Gaur, N., Steinbach, R., Witte, O.W., Grosskreutz, J., 2020. Modelling disease course in amyotrophic lateral Sclerosis: pseudo-longitudinal insights from cross-sectional health-related quality of life data. *Health Qual Life Outcomes* 18, 117.
- Schuster, C., Kasper, E., Machts, J., Bittner, D., Kaufmann, J., Benecke, R., Teipel, S., Vielhaber, S., Prudlo, J., 2013. Focal thinning of the motor cortex mirrors clinical features of amyotrophic lateral sclerosis and their phenotypes: a neuroimaging study. *J. Neurol.* 260 (11), 2856–2864.
- Schuster, C., Kasper, E., Machts, J., Bittner, D., Kaufmann, J., Benecke, R., Teipel, S., Vielhaber, S., Prudlo, J., 2014. Longitudinal course of cortical thickness decline in amyotrophic lateral sclerosis. *J. Neurol.* 261 (10), 1871–1880.
- Seiger, R., Ganger, S., Kranz, G.S., Hahn, A., Lanzenberg, R., 2018. Cortical thickness estimations of FreeSurfer and the CAT12 toolbox in patients with alzheimer's disease and healthy controls. *J. Neuroimaging* 28 (5), 515–523.
- Senda, J., Atsuta, N., Watanabe, H., Bagarinao, E., Imai, K., Yokoi, D., Riku, Y., Masuda, M., Nakamura, R., Watanabe, H., Ito, M., Katsuno, M., Naganawa, S., Sobue, G., 2017. Structural MRI correlates of amyotrophic lateral sclerosis progression. *J. Neurol. Neurosurg. Psychiatry* 88 (11), 901–907.
- Sicotte, N.L., Voskuhl, R.R., Bouvier, S., Klutzh, R., Cohen, M.S., Maziotta, J.C., 2003. Comparison of multiple sclerosis lesions at 1.5 and 3.0 Tesla. *Invest. Radiol.* 38, 423–427.
- Sorenson, E.J., Mandrekar, J., Crum, B., Stevens, J.C., 2007. Effect of referral bias on assessing survival in ALS. *Neurology* 68 (8), 600–602.
- Spalthoff, R., Gaser, C., Nenadic, I., 2018. Altered gyrification in schizophrenia and its relation to other morphometric markers. *Schizophr. Res.* 202, 195–202.
- Spinnelli, E.G., Agosta, F., Ferraro, P.M., Riva, N., Lunetta, C., Falzone, Y.M., Comi, G., Falini, A., Filippi, M., 2016. Brain MR imaging in patients with lower motor neuron-predominant disease. *Radiology* 280 (2), 545–556.
- Spinnelli, E.G., Riva, N., Rancoita, P.M.V., Schito, P., Doretti, A., Poletti, B., Di Serio, C., Silani, V., Filippi, M., Agosta, F., 2020. Structural MRI outcomes and predictors of disease progression in amyotrophic lateral sclerosis. *Neuroimage Clin.* 27, 102315.
- Steinbach, R., Gaur, N., Stubendorff, B., Witte, O.W., Grosskreutz, J., 2018. Developing a neuroimaging biomarker for amyotrophic lateral sclerosis: multi-center data sharing and the road to a "global cohort". *Front. Neurol.* 9, 1055.
- Steinbach, R., Batrybekova, M., Gaur, N., Voss, A., Stubendorff, B., Mayer, T.E., Gaser, C., Witte, O.W., Prell, T., Grosskreutz, J., 2020. Applying the D50 disease progression model to gray and white matter pathology in amyotrophic lateral sclerosis. *Neuroimage Clin.* 25, 102094.
- Steinbach, R., Gaur, N., Roediger, A., Mayer, T.E., Witte, O.W., Prell, T., Grosskreutz, J., 2021a. Disease aggressiveness signatures of amyotrophic lateral sclerosis in white matter tracts revealed by the D50 disease progression model. *Hum. Brain Mapp.* 42, 737–752.
- Steinbach, R., Prell, T., Gaur, N., Roediger, A., Gaser, C., Mayer, T.E., Witte, O.W., Grosskreutz, J., 2021b. Patterns of grey and white matter changes differ between bulbar and limb onset amyotrophic lateral sclerosis. *Neuroimage Clin.* 30, 102674.
- Thakore, N.J., Lapin, B.R., Pioro, E.P., Pooled Resource Open-Access, A.L.S.C.T.C., 2018. Trajectories of impairment in amyotrophic lateral sclerosis: Insights from the Pooled Resource Open-Access ALS Clinical Trials cohort. *Muscle Nerve* 57, 937–945.
- Tullo, S., Devenyi, G.A., Patel, R., Park, M.T.M., Collins, D.L., Chakravarty, M.M., 2018. Warping an atlas derived from serial histology to 5 high-resolution MRIs. *Sci. Data* 5, 180107.
- Turner, M.R., Grosskreutz, J., Kassubek, J., Abrahams, S., Agosta, F., Benatar, M., Filippi, M., Goldstein, L.H., van den Heuvel, M., Kalra, S., Lule, D., Mohammadi, B., first Neuroimaging Symposium in, A.L.S., 2011. Towards a neuroimaging biomarker for amyotrophic lateral sclerosis. *Lancet Neurol* 10, 400–403.
- Turner, M.R., Verstraete, E., 2015. What does imaging reveal about the pathology of amyotrophic lateral sclerosis? *Curr. Neurol. Neurosci. Rep.* 15, 45.
- Turner, M.R., Agosta, F., Bede, P., Govind, V., Lulé, D., Verstraete, E., 2012. Neuroimaging in amyotrophic lateral sclerosis. *Biomark Med.* 6 (3), 319–337.
- van der Burgh, H.K., Westenberg, H.-J., Walhout, R., van Veenhuijzen, K., Tan, H.H.G., Meier, J.M., Bakker, L.A., Hendrikse, J., van Es, M.A., Veldink, J.H., van den Heuvel, M.P., van den Berg, L.H., 2020. Multimodal longitudinal study of structural brain involvement in amyotrophic lateral sclerosis. *Neurology* 94 (24), e2592–e2604.
- van Es, M.A., Hardiman, O., Chio, A., Al-Chalabi, A., Pasterkamp, R.J., Veldink, J.H., van den Berg, L.H., 2017. Amyotrophic lateral sclerosis. *Lancet* 390 (10107), 2084–2098.
- Verstraete, E., van den Heuvel, M.P., Veldink, J.H., Blanken, N., Mandl, R.C., Hulshoff Pol, H.E., van den Berg, L.H., Zhan, W., 2010. Motor network degeneration in amyotrophic lateral sclerosis: a structural and functional connectivity study. *PLoS ONE* 5 (10), e13664.
- Verstraete, E., Veldink, J.H., Hendrikse, J., Schelhaas, H.J., van den Heuvel, M.P., van den Berg, L.H., 2012. Structural MRI reveals cortical thinning in amyotrophic lateral sclerosis. *J. Neurol. Neurosurg. Psychiatry* 83 (4), 383–388.
- Verstraete, E., Turner, M.R., Grosskreutz, J., Filippi, M., Benatar, M., 2015. Mind the gap: the mismatch between clinical and imaging metrics in ALS. *Amyotroph. Lateral Scler. Frontotemporal Degener.* 16 (7–8), 524–529.
- Westenberg, H.-J., Verstraete, E., Walhout, R., Schmidt, R., Hendrikse, J., Veldink, J.H., van den Heuvel, M.P., van den Berg, L.H., 2015. Subcortical structures in amyotrophic lateral sclerosis. *Neurobiol. Aging* 36 (2), 1075–1082.
- Westenberg, H.-J., Debray, T.P.A., Visser, A.E., van Eijk, R.P.A., Rooney, J.P.K., Calvo, A., Martin, S., McDermott, C.J., Thompson, A.G., Pinto, S., Kobleva, X., Rosenbohm, A., Stubendorff, B., Sommer, H., Middelkoop, B.M., Dekker, A.M., van Vugt, J.J.F.A., van Rheenen, W., Vajda, A., Heverin, M., Kazoka, M., Hollinger, H., Gromicho, M.,

Körner, S., Ringer, T.M., Rödiger, A., Gunkel, A., Shaw, C.E., Bredenoord, A.L., van Es, M.A., Corcia, P., Couratier, P., Weber, M., Grosskreutz, J., Ludolph, A.C., Petri, S., de Carvalho, M., Van Damme, P., Talbot, K., Turner, M.R., Shaw, P.J., Al-Chalabi, A., Chiò, A., Hardiman, O., Moons, K.G.M., Veldink, J.H., van den Berg, L.H., 2018.

Prognosis for patients with amyotrophic lateral sclerosis: development and validation of a personalised prediction model. *Lancet Neurol.* 17 (5), 423–433.

Winterburn, J.L., Pruessner, J.C., Chavez, S., Schira, M.M., Lobaugh, N.J., Voineskos, A. N., Chakravarty, M.M., 2013. A novel in vivo atlas of human hippocampal subfields using high-resolution 3 T magnetic resonance imaging. *Neuroimage* 74, 254–265.

Woo, C.W., Krishnan, A., Wager, T.D., 2014. Cluster-extent based thresholding in fMRI analyses: pitfalls and recommendations. *Neuroimage* 91, 412–419.